Polymer Journal (2010) 42, 342–348

www.nature.com/pj

ORIGINAL ARTICLE

Synthesis and characterization of cellulose-*b*-polystyrene

Shunsuke Yagi[1], Natsuki Kasuya[2] and Kiyoharu Fukuda[2]

A block copolymer of cellulose and polystyrene (PS) was synthesized through atom transfer radical polymerization. Macroinitiators (MIs) were prepared by introducing 2-chloroacetamide to the reducing end of cellulose (degree of polymerization=20, 50, 250). Subsequently, MIs were copolymerized with styrene monomer in a system of *N,N,N′,N″,N″*-pentamethyldiethylenetriamine/CuCl or CuBr/ascorbic acid at 130 °C. The resulting copolymers were characterized by ^{1}H nuclear magnetic resonance and size-exclusion chromatography. The kinetic study indicated that the polymerization was controllable. The efficacy of copolymers in compatibilizing an immiscible cellulose/PS blend was confirmed by microscopic observation. The mechanism of thermal and thermo-oxidative decomposition of the blend was investigated by thermogravimetry.
Polymer Journal (2010) **42,** 342–348; doi:10.1038/pj.2009.342; published online 10 February 2010

Keywords: ATRP; block copolymer; cellulose; polymer blend; polystyrene; thermogravimetry

INTRODUCTION

Cellulose is gaining attention as a fuel alternative to fossil resources because it is one of the most abundant natural organic resources and is renewable. In addition to its potential use as a sustainable resource for fuels such as bio-ethanol and bio-methanol, it is also gaining attention as an option for biomass-based polymeric materials.[1] Biomass-based polymers seem promising for a post-petroleum era, whether they are prepared by polymer reaction or polymerization.

So far, most of the industrial modifications of cellulose (that is, cellulose derivatives) to improve its properties have been cellulose esters, ethers and graft copolymers, obtained by changing the hydroxyl groups of the cellulose molecules. Among these derivatives, the applications of cellulosic graft copolymers have been mainly in the textile field. However, copolymers in general have a variety of uses, such as stimuli–responsive (for example, pH, light, electric field, magnetic field, ionic strength) polymers,[2–5] biodegradable polymers,[4,6,7] surfactants,[8] compatibilizers[9] and so on. Cellulosic copolymers are also expected to possess these interesting properties and be used in fields other than textiles. In particular, as copolymers are known to be good compatibilizers for polymer alloys, we expect cellulosic copolymers to be good compatibilizers.

When two or more homopolymers are blended, the components often separate into two or more phases. However, by adding a good compatibilizer, such a blend can suppress separation by reducing interfacial tension, and the resulting blend may obtain new properties. Among the copolymers used as compatibilizers, block copolymer is reportedly superior to graft copolymer; moreover, high-molecular-weight diblock copolymers with a balanced composition (symmetrical) exhibit even better compatibilization ability.[10]

In addition to the studies of block copolymers as compatibilizers, much recent work has focused on the self-assembling properties of amphiphilic block copolymers for use as emulsifiers in drug delivery systems.[5,8,11] In drug delivery systems, hydrophobic drugs are entrapped in the core of block copolymer micelles. Generally, the aggregation properties of micelles, such as the average molar mass of aggregates and the aggregation numbers, are related to the degree of polymerization (DP) of each block domain; therefore, it is possible to optimize the solubility and stability of micelles by adjusting the DP of each block domain.

Thus, block copolymer has great potential to produce novel materials with unique properties.[12] However, there are few papers on cellulosic block copolymers,[13] in contrast to a large number of papers on cellulosic graft copolymers.[14–18]

We synthesized cellulose-*b*-polystyrene by atom transfer radical polymerization (ATRP), a method that was developed by Wang and Matyjaszewski[19,20] and by Kato *et al.*[21] This method is useful for preparing polymers with controlled molecular weight, polydispersity, composition and topology. It is also applicable to various combinations of vinyl monomers and solvents.[22–26]

Our aim was to synthesize cellulosic block copolymer and to evaluate the applicability of the copolymer as a compatibilizer of cellulose/PS blends. Macroinitiators (MIs) were synthesized from cellulose (DP=20, 50 and 250). The copolymers obtained were characterized by ^{1}H nuclear magnetic resonance (NMR) spectroscopy and size-exclusion chromatography (SEC). The kinetics of copolymer-

[1]Department of Natural Resources and Ecomaterials, Graduate School of Agriculture, Tokyo University of Agriculture and Technology, Saiwai-cho, Fuchu, Japan and [2]Institute of Symbiotic Science and Technology, Tokyo University of Agriculture and Technology, Saiwai-cho, Fuchu, Japan
Correspondence: S Yagi, Natural Resources and Ecomaterials, Tokyo University of Agriculture and Technology, 3-5-8 Saiwai-cho, Fuchu, Tokyo 183-8509, Japan.
E-mail: syagi@e-mail.jp
Received 14 October 2009; revised 16 December 2009; accepted 18 December 2009; published online 10 February 2010

ization were analyzed using gas chromatography. The compatibilizing effect of cellulose-*b*-polystyrene on cellulose/polystyrene (PS) blends was observed using a microscope. The thermal properties of blend samples were characterized by thermogravimetry (TG).

EXPERIMENTAL PROCEDURE

Materials

Cellulose (CF11; Whatman, Maidstone, UK) was used as received. Tencel fiber was donated by Lenzing Japan's marketing office. Styrene (St; 99.9%, Wako, Osaka, Japan) was passed through a column filled with alumina and then distilled under reduced pressure. 2,2′-Azobis(isobutyronitrile) (98.0%, Wako), copper(I) chloride (CuCl; 99.9%, Wako), copper(I) bromide (CuBr; 95.0%, Wako), L-(+)-ascorbic acid (AA; 99.5%, Wako), *N,N,N′,N″,N″*-pentamethyldiethylenetriamine (PMDETA; 98.0%, Wako), 2-chloroacetamide (CAA; 97.0%, Tokyo Kasei, Tokyo, Japan), sodium cyanoborohydride ($NaBH_3CN$; 95%, Aldrich, St Louis, MO, USA), *N,N*-dimethylacetamide (DMAc; 98.0%, Wako), lithium chloride (LiCl; 99.0%, Wako), methanol (99.5%, Wako), tetrahydrofuran (THF; 99.5%, Wako), phenyl isocyanate (98.0%, Wako), *N,N*-dimethyl-4-aminopyridine (99.9%, Wako), acetic anhydride (97.0%, Wako), pyridine (99.5%, Wako), hydrochloric acid (HCl; 35–37%, Wako) and phosphoric acid (85%, Wako) were used as received.

Characterization

NMR spectra were recorded on a JEOL (Tokyo, Japan) alpha600 NMR spectrometer. Molecular weights and molecular-weight distributions were measured by SEC on a high-performance liquid chromatography system with a GL Sciences (Tokyo, Japan) PU610-1X pump, two serial columns (TSKgel $G2500H_{XL}$ and TSKgel $G4000H_{XL}$) and a UV620 detector. THF was used as eluent, flowing at 0.5 ml min^{-1} at 25 °C. PS standards were used for calibration. Monomer conversion was determined by gas chromatography (GC353B; GL Sciences) with a flame ionization detector and a capillary column 30QC2/BPX70 (SGE, Melbourne, Vic, Australia). 1,4-Dibromobenzene was used as an internal standard for the gas chromatography. The morphology of the blend films was observed using an optical microscope (BX51; Olympus, Tokyo, Japan). Thermal degradation was investigated with a simultaneous TG/DTG instrument (DTG-60/60H; Shimadzu, Kyoto, Japan). Measurements were conducted at heating rates of 5, 8, 10 and 20 °C min^{-1} in He or air. The activation energies of thermal decomposition were estimated by applying the Friedman,[27] Ozawa,[28] Kissinger–Akahira–Sunose (KAS)[29,30] and Coats–Redfern methods.[31] The chlorine content of MI was evaluated by the oxygen flask combustion method.

Hydrolysis of cellulose by phosphoric acid (cellulose$_{20}$)

Microcrystalline cellulose powder (CF11; Whatman) was hydrolyzed with phosphoric acid as reported by Isogai and Usuda.[32] CF11 (50 g) was immersed in a mixture of water (36 ml) and 85% phosphoric acid (935 ml) at room temperature for 4 weeks. The obtained cellulose solution was poured into a large amount of water, and the precipitate was collected by centrifugation, washed with water and methanol repeatedly and dried *in vacuo* at 40 °C.

Hydrolysis of cellulose by hydrochloric acid (cellulose$_{50}$)

Tencel fiber (31 g) was added to a mixture of water (516 ml) and hydrochloric acid (83 ml) and heated under refluxing for 2.5 h with stirring. The resulting cellulose suspension was poured into a large amount of water, and the precipitate was collected by centrifugation, washed with water and methanol repeatedly and dried *in vacuo* at 40 °C.

Procedures for the preparation of cellulose-*Cl*

Cellulose (5 g) was dispersed in DMAc (100 ml), and the suspension was stirred under refluxing for 0.5 h at 165 °C. Thereafter, LiCl (8 g) was added, and the mixture was stirred constantly overnight at room temperature until it became a clear solution. Into the solution were added $NaBH_3CN$ (0.1 g) and CAA (3.8 g for cellulose$_{20}$, 1.2 g for cellulose$_{50}$, 0.23 g for CF11), followed by stirring at 70 °C for 24 h. The resulting solution was poured into a large amount of water, and the resulting precipitate was filtered, washed with water and methanol repeatedly and dried *in vacuo* at 40 °C.

Procedures for the synthesis of cellulose-*b*-PS

MIs were added to a volume of DMAc equal to the volume of St and heated under refluxing for 0.5 h at 165 °C with stirring. Thereafter, LiCl was added, and the mixture was stirred overnight at room temperature to obtain a transparent solution. In a two-necked flask, the following were added to the resulting solution: St, CuCl (or CuBr), PMDETA and AA. After sealing the flask with a rubber septum, a cycle of gas evacuation and nitrogen filling was repeated three times to remove oxygen. The mixture was then heated at 130 °C with stirring. Small aliquots of the sample were taken periodically to monitor the polymerization process. These were diluted with THF and passed through a column filled with alumina before analysis by gas chromatography. After the elapse of a predetermined amount of time, the reaction mixture was poured into a large amount of methanol, and the resulting precipitate was filtered, washed with methanol repeatedly and dried *in vacuo* at 40 °C.

Acetylation of cellulose$_{250}$-*b*-PS

Before acetylation, the crude cellulose$_{250}$-*b*-PS was washed with THF and dried *in vacuo* at 40 °C. The resulting copolymer (0.8 g) was immersed in pyridine (15 ml) overnight. *N,N*-Dimethyl-4-aminopyridine (0.01 g) and acetic anhydride (5 ml) were added to the suspension, and the mixture was stirred for 40 h at room temperature. The mixture was then poured into a large amount of methanol, and the resulting precipitate was filtered, washed with water and methanol repeatedly and dried *in vacuo* at 40 °C.

Carbanilation of cellulose-*b*-PS

Cellulose-*b*-PS (0.2 g) was immersed in pyridine (15 ml) overnight. Phenyl isocyanate (2 ml) was then added, and the mixture was stirred at 70 °C for 40 h. Methanol was added to the solution to degrade the excess phenyl isocyanate, and then the solvent, including methanol, was removed by evaporation. The crude product was washed with water and methanol repeatedly and dried *in vacuo* at 40 °C.

Procedures for the synthesis of PS for the cellulose/PS blends

The PS homopolymer was prepared by radical polymerization. 2,2′-Azobis (isobutyronitrile) (0.1 g) and St monomer (50 ml) were added to a reaction container. After sealing it with a rubber septum, a cycle of gas evacuation and nitrogen filling was repeated three times to remove oxygen. The solution was then heated at 130 °C for 7 h. After polymerization, the resulting polymer was dissolved in THF and then precipitated in a large amount of methanol. The resulting precipitate was filtered, washed with methanol repeatedly and dried *in vacuo* at 40 °C. The weight-average molecular weight and polydispersity were 160 000 and 2.29, respectively.

Blend films preparation for microscopic observations

Cellulose (CF11; Whatman), PS and cellulose$_{20}$-*b*-PS (M_w=42 000) were dissolved in LiCl/DMAc each. Each clear solution was mixed at an arbitrary composition. The obtained mixture solutions were cast on glass plates and rinsed in water. The blend films were then observed using a microscope.

Blend preparation for TG analysis

Cellulose/PS/cellulose-*b*-PS blends (5/5/0 and 4/4/2 by weight) were prepared as follows: Cellulose (CF11; Whatman), PS and cellulose$_{20}$-*b*-PS (M_w=42 000) were dissolved in LiCl/DMAc each. Each clear solution was mixed at an arbitrary composition, and then precipitated in a large amount of water. The resulting precipitate was filtered and dried *in vacuo* at 40 °C.

RESULTS AND DISCUSSION

Synthesis of cellulose-*b*-PS block copolymer

Scheme 1 shows the synthetic procedures of cellulose-*b*-PS. We prepared the MI for the first step by introducing CAA to the reducing ends of cellulose. The formyl group in the cellulose reducing end and the amino group of the CAA reacted to form a Schiff base, which was then reduced with $NaBH_3CN$. The obtained MI (cellulose-*Cl*) was copolymerized with St monomer. Cellulose$_{250}$-*Cl* was copolymerized using CuBr, whereas cellulose$_{20}$-*Cl* and cellulose$_{50}$-*Cl* were copolymerized using CuCl.

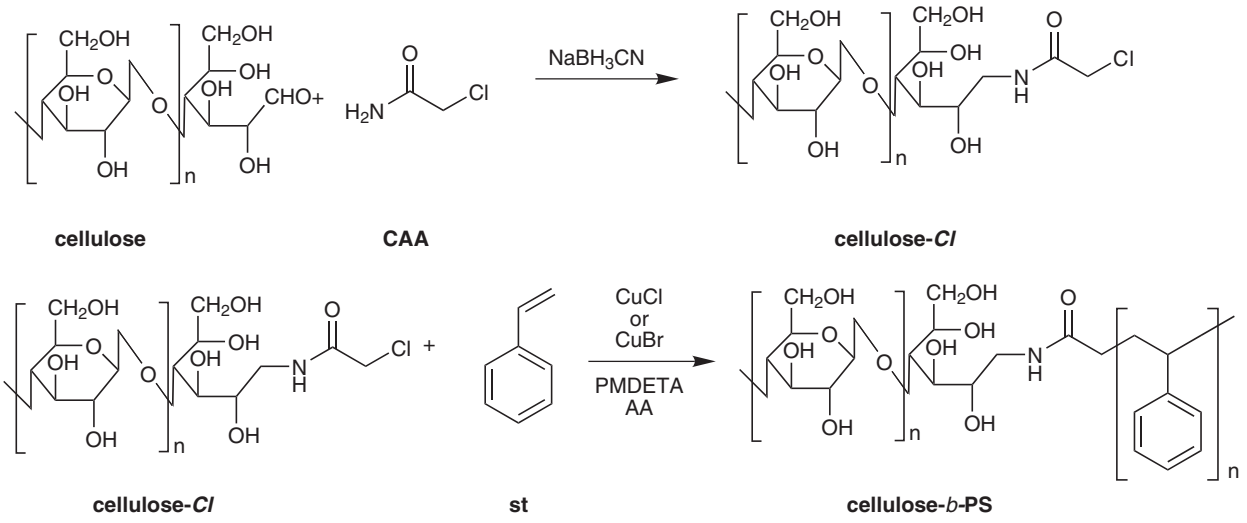

Scheme 1 Synthetic procedures for cellulose-*b*-PS.

In typical ATRP, the polymerization rate increases with initiator concentration. In copolymerization using cellulose$_{250}$-*Cl*, however, it is difficult to prepare MI solution with a concentration high enough to achieve a sufficient polymerization rate. Therefore, we used CuBr as the catalyst instead of CuCl because halogen exchange enhances the polymerization rate. Growing chains capped with Br have a higher propagation rate and better polydispersity than those capped with Cl. These effects are thought to be due to low bond-dissociation energy of Br.[22]

Characterization of MI (cellulose-*Cl*)

Table 1 shows the number-average molecular weight (M_n), the weight-average molecular weight (M_w) and the polydispersity (M_w/M_n) of MI, which were phenylcarbanilated before SEC for ultraviolet detection. Although previous work by Isogai and Usuda[32] showed that DP and the polydispersity of cellulose hydrolyzed with phosphoric acid were 15.5 and 1.15, respectively, DP and the polydispersity of our cellulose$_{20}$-*Cl* prepared using cellulose hydrolyzed under similar conditions as Isogai and Usuda,[32] were 20 and 1.67, respectively, suggesting insufficient hydrolysis of cellulose.

The amounts of CAA incorporated were evaluated by oxygen flask combustion. The percentages of the modified reducing terminals for cellulose$_{20}$ and cellulose$_{50}$ were estimated to be 57 and 41%, respectively. Chlorine incorporation was undetectable for cellulose$_{250}$ by the method. These MIs were copolymerized with styrene.

Kinetic study of cellulose-*b*-PS block copolymer

Kinetics for the copolymerization of St with cellulose$_{20}$-*Cl* as an MI were also investigated (Figure 1). The relationship between monomer concentration and radical concentration is as follows.

$$\ln \frac{[M]_0}{[M]_t} = k_p[P^*]t, \quad (1)$$

where t is the time, $[M]_t$ is the monomer concentration at t, $[M]_0$ is the initial monomer concentration, k_p is the propagation constant and $[P^*]$ is the concentration of the active propagating species.

The straight semilogarithmic kinetic plot for $\ln([M]_0/[M]_t)$ and the linear plot of conversion vs time t indicate that the copolymerization of St was on the first order with respect to reaction time when the conversion of monomer was not very high. This suggests that the concentration of growing radicals remained constant during polymerization. Similar results were obtained from copolymerizaton with the other MI. Our method enables us to design and produce cellulose-*b*-PS with a predetermined molecular weight of PS block.

Table 1 Molecular weights, polydispersity and degree of polymerization (DP) of phenyl carbanilated macroinitiators

Sample	M_n	M_w	M_w/M_n	*DP*
Cellulose$_{20}$-*Cl*	6000	10 000	1.67	20
Cellulose$_{50}$-*Cl*	14 000	24 000	1.71	50
Cellulose$_{250}$-*Cl*	85 000	130 000	1.53	250

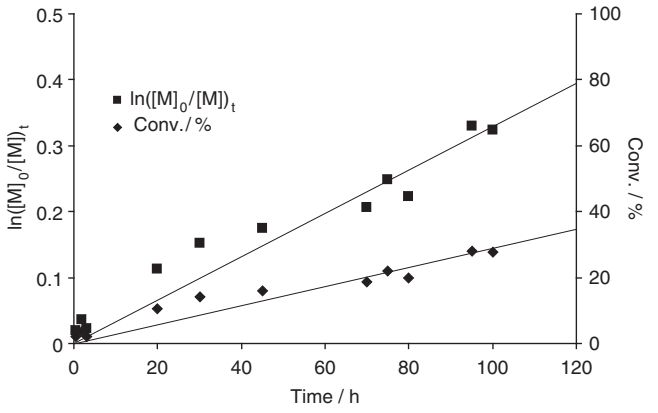

Figure 1 Kinetic plot for the copolymerization of St in the presence of MI (DP=20): MI=0.2 g, St=20 ml, [St]:[CuCl]:[AA]:[PMDETA]=300:1:0.5:3.

^{1}H NMR spectrum of cellulose-*b*-PS block copolymer

The ^{1}H NMR spectrum for the resulting polymer was measured after displacing the hydroxyl groups in cellulose with acetyl groups to enhance the polymer's solubility in the solvent ($CDCl_3$) (Figure 2). The broad signals at 1.2–1.6 p.p.m. (a) were assigned to the methylene protons in the PS main chain (-CH_2-), and those at 1.7–2.2 p.p.m. (b) were assigned to the methine proton in the PS main chain (-CH-).

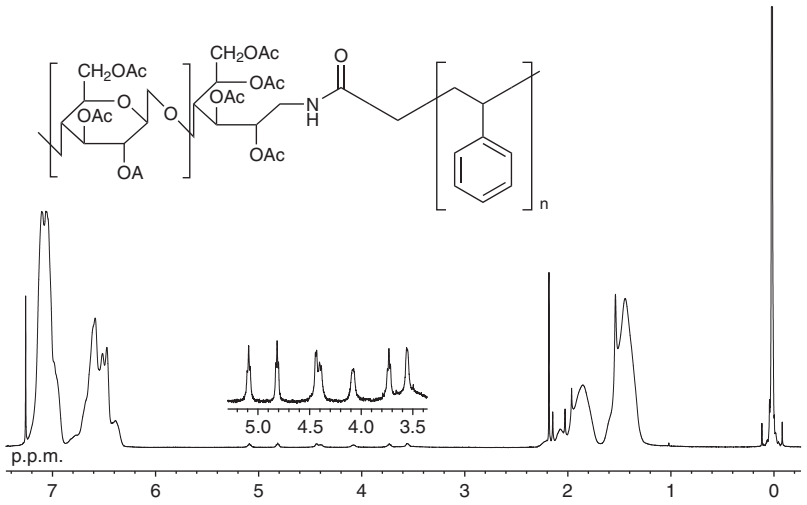

Figure 2 ^{1}H NMR spectrum of acetylated cellulose$_{250}$-*b*-PS obtained under the following conditions: MI (cellulose$_{250}$-*Cl*)=0.2 g, St=13 ml, [St]:[CuBr]:[AA]:[PMDETA]=250:1:0.5:1, polymerization time=50 h.

Sharp peaks at 1.97, 2.02 and 2.13 p.p.m. in this region were assigned to the methyl protons of the acetyl group (-$COCH_3$), and signals at 2.2 p.p.m. were due to PMDETA. In addition, the signals at 6.4–7.2 p.p.m. (c), 3.5–5.2 p.p.m. (H-5: 3.6 p.p.m., H-4: 3.7 p.p.m., H-6: 4.2 and 4.4 p.p.m., H-1: 4.5 p.p.m., H-2: 4.8 p.p.m., H-3: 5.1 p.p.m.) were assigned to aromatic protons and to protons bonding directly to the glucose ring, respectively. The PS indicated in Figure 2 was assumed to link covalently to cellulose, as, before acetylation for NMR measurement, pure PS (homo-PS) was removed by washing with THF, which is a good solvent for PS but not for cellulose.

SEC of cellulose-*b*-PS block copolymer

SECs for phenylcarbanilated cellulose-*b*-PS are shown in Figure 3. As these original chromatograms (dotted line) indicate a bimodal distribution, we deconvoluted the chromatograms (solid line).

The molecular weights of phenylcarbanilated cellulose-*b*-PS calculated using Figure 3 are listed in Table 2. The M_w of the lower-molecular-weight peak in Figure 3a was 8000; this value is close to the M_w of phenylcarbanilated MI (cellulose$_{20}$-*Cl* in Table 1). This peak stayed at the same position even when the polymerization time was prolonged. Similarly, the M_w of the lower-molecular-weight peaks in Figures 3b and c was close to the corresponding values for their MI, and these peaks stayed at the same position even after repeated polymerization. The M_n follows a similar pattern except for cellulose$_{20}$.

These results suggest that the lower-molecular-weight peaks in Figure 3 were obtained from the phenylcarbamate of the remaining original cellulose, getting rid of the incorporation of CAA at the reducing terminals, or from the phenylcarbamate of MI with its terminal inactivated toward ATRP. The insufficient incorporation of CAA was probably due to the low nucleophilicity of nitrogen atoms in CAA.

On the other hand, the higher-molecular-weight peaks in Figure 3 were attributed to phenylcarbamates of cellulose-*b*-PS, because these peaks shifted to a higher-molecular-weight region with increasing polymerization time. Consequently, the M_w and the polydispersity for phenylcarbamate of cellulose$_{20}$-*b*-PS were estimated to be 49 000 and 1.75, those of cellulose$_{50}$-*b*-PS were 130 000 and 1.97 and those of cellulose$_{250}$-*b*-PS were 350 000 and 1.25, respectively. The narrow polydispersity of cellulose$_{250}$-*b*-PS probably resulted from the activated growing chains capped with Br.[22]

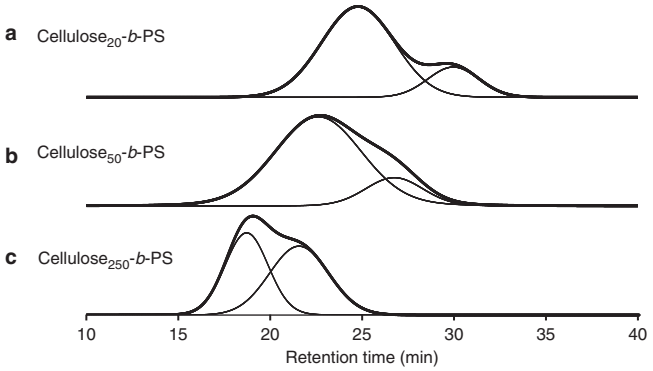

Figure 3 SEC traces before (dotted line) and after deconvolution (solid line) of phenylcarbanilated cellulose-*b*-PS. Conditions for polymerization were as follows: (**a**) MI (cellulose$_{20}$-*Cl*)=0.2 g, St=13 ml, [St]:[CuCl]:[AA]:[PMDETA]=1400:1:0.5:1, polymerization time=5 h, (**b**) MI (cellulose$_{50}$-*Cl*)=0.2 g, St=13 ml, [St]:[CuCl]:[AA]:[PMDETA]=400:1:0.5:1, polymerization time=20 h, (**c**) MI (cellulose$_{250}$-*Cl*)=0.2 g, St=13 ml, [St]:[CuBr]:[AA]:[PMDETA]=250:1:0.5:1, polymerization time=20 h.

Table 2 Evaluation of SEC traces after deconvolution of phenylcarbanilated cellulose-*b*-PS

Sample	M_n	M_w	M_w/M_n
Cellulose$_{20}$-*b*-PS	28 000	49 000	1.75
	3500	8000	2.29
Cellulose$_{50}$-*b*-PS	66 000	130 000	1.97
	14 000	20 000	1.43
Cellulose$_{250}$-*b*-PS	280 000	350 000	1.25
	79 000	120 000	1.52

Abbreviations: PS, polystyrene; SEC, size-exclusion chromatography.

Microscopic observation of blend films

The improvement of cellulose/PS compatibility caused by the addition of cellulose-*b*-PS was investigated using an optical microscope. Figure 4 shows micrographs of cellulose/PS/cellulose$_{20}$-*b*-PS blend films

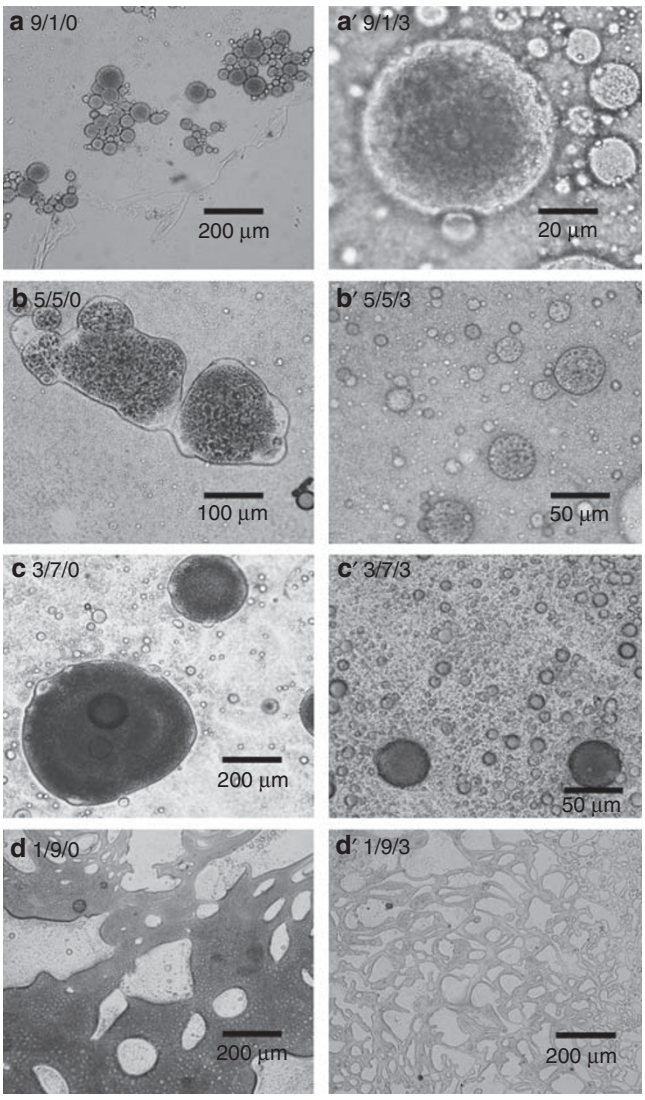

Figure 4 Micrographs of cellulose/PS/cellulose$_{20}$-*b*-PS. The weight ratios of the components are (**a**) 9/1/0, (**a′**) 9/1/3, (**b**) 5/5/0, (**b′**) 5/5/3, (**c**) 3/7/0, (**c′**) 3/7/3, (**d**) 1/9/0 and (**d′**) 1/9/3.

prepared by casting solution, followed by water displacement. The bright regions are cellulose and the dark regions are PS.

As the amount of PS increased, the PS domains in uncompatibilized films (Figures 4a–c) readily aggregated and coalesced. In contrast, the PS domains in compatibilized films were dispersed and stayed relatively small (Figures 4a′–c′). At higher concentrations of PS (Figures 4d and d′), phase separation was suppressed to some extent by the addition of cellulose$_{20}$-*b*-PS. These observations show the potential of cellulose-*b*-PS as a compatibilizer.

TG analysis of blend samples

Figures 5–7 show TG curves for each sample. Table 3 shows initial decomposition temperatures of blends at 5% weight loss. It indicates that the thermal stability of the cellulose/PS blend was decreased by the addition of cellulose-*b*-PS. Nishioka *et al.*[33] also reported a decline in thermal stability for blend systems composed of cellulose, hydrophobic poly(methyl acrylate) and cellulose-*g*-poly(methyl acrylate). They have hypothesized that the crystallinity of cellulose was decreased by the proximity of synthetic polymer, which decreases the thermal stability of the blend.

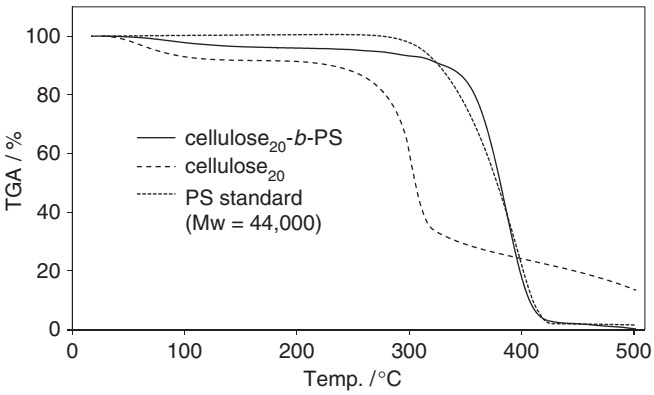

Figure 5 TG curves of cellulose$_{20}$-*b*-PS (M_w=42 000), cellulose$_{20}$ and PS standard (M_w=44 000) at 10 °C min^{-1} under He.

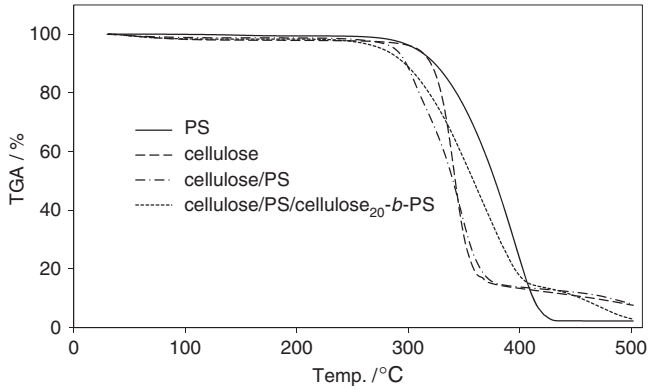

Figure 6 TG curves of PS, cellulose (CF11), cellulose (CF11)/PS and cellulose (CF11)/PS/cellulose$_{20}$-*b*-PS at 10 °C min^{-1} under He.

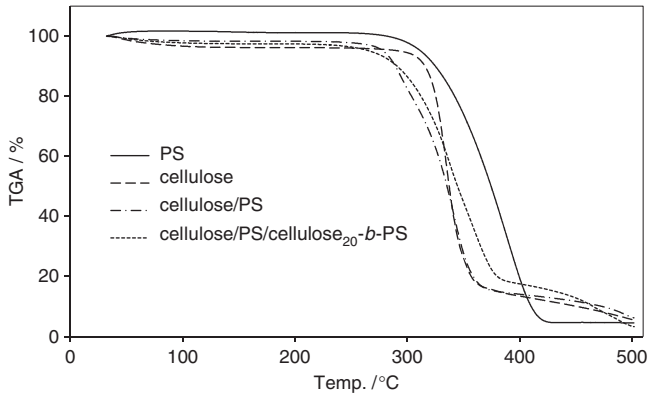

Figure 7 TG curves of PS, cellulose (CF11), cellulose (CF11)/PS and cellulose (CF11)/PS/cellulose$_{20}$-*b*-PS at 10 °C min^{-1} under air.

We studied the kinetics of thermal and thermo-oxidative degradation of blends by following methods reported elsewhere.[34–38] We were able to determine the thermal decomposition process by comparing the activation energy (E_a) calculated by model-free methods[27–30] with the E_a calculated by the Coats–Redfern method[31] with different models.[34–38] Table 4 shows the E_a of thermal decomposition calculated

Table 3 Initial decomposition (5% weight loss) temperatures (°C) of blends

	Cellulose/PS		*Cellulose/PS/cellulose-b-PS*	
Heating rate (°C min^{-1})	*He*	*Air*	*He*	*Air*
5	277	264	199	261
8	270	273	267	262
10	288	279	277	267
20	303	292	281	269

Abbreviation: PS, polystyrene.

Table 4 E_a of each sample calculated by model-free methods ($0 < \alpha \leqq 0.2$)

Method	*Atmosphere*	*Cellulose (kJ mol^{-1})*	*PS (kJ mol^{-1})*	*Cellulose/PS (kJ mol^{-1})*	*Cellulose/PS/ cellulose-b-PS (kJ mol^{-1})*
Friedman	He	189	137	115	101
	Air	156	65	123	156
Ozawa	He	191	137	113	101
	Air	157	70	124	159
KAS	He	191	134	110	97
	Air	155	64	122	158

Abbreviation: PS, polystyrene.

using model-free methods (Friedman,[27] Ozawa[28] and KAS[29,30]). There were no major differences among the different methods.

The E_a of thermal decomposition of each blend was also calculated by the Coats–Redfern method. (Detailed calculations were omitted.) These calculations show that the most probable mechanisms for thermal and thermo-oxidative degradation of the cellulose/PS blend are random nucleation and nuclei growth ($A_{1.5}$ model; Avrami–Erofeev equation, Avrami exponent n=1.5) and phase boundary controlled reaction (R_1 model; one-dimensional movement), respectively. The thermal and thermo-oxidative degradation mechanisms of the cellulose/PS/cellulose-*b*-PS blend are random nucleation and nuclei growth (A_1 model; Avrami–Erofeev equation, Avrami exponent n=1) and two-dimensional diffusion (D_2 model; Valensi equation.), respectively.

The Avrami exponent (n) contains information about nucleation and nuclei growth. A lower n value indicates lower-dimensional nuclei growth. Therefore, it can be concluded that the direction of nuclei growth of the cellulose/PS/cellulose-*b*-PS blend (A_1 model) was restricted compared with that of the cellulose/PS blend ($A_{1.5}$ model). Considering the fact that cellulose-*b*-PS has a tendency to localize around the interface of the polymer blend, it is possible that thermal decomposition of the cellulose/PS/cellulose-*b*-PS blend progressed along the blend interface at the initial decomposition stage. We hypothesize that the lower n value reflects the preferential degradation of thermolabile cellulose-*b*-PS along the blend interface. Furthermore, it is also possible that the increasing area of the reactive interfacial site caused the higher nucleation rate and the decline in thermal stability of the cellulose/PS/cellulose-*b*-PS blend.

The R and D models assume a contracting interfacial reaction, whereas the A model assumes a growing interfacial reaction. Therefore, we concluded that thermo-oxidative degradation started from the surface. In addition, the rate-controlling step of the R model is chemical reactions, such as the bond scission reaction, whereas the rate-controlling step of the D model is the diffusion of chemical species such as oxygen and radicals. We hypothesize that cellulose-*b*-PS, which is localized around the surface of PS particles, decomposed easily when the reactive interface reached around the PS interface. Therefore, the thermo-oxidative decomposition of the cellulose/PS/cellulose-*b*-PS blend was the diffusion-controlling mechanism (D_2 model).

For these reasons, we attribute the decline in the initial thermal stability caused by the addition of cellulose-*b*-PS to the preferential decomposition of thermolabile cellulose-*b*-PS and to the increase in interfacial area as a reaction site.

CONCLUSION

Cellulose-*b*-PS copolymers were synthesized by ATRP. MIs were prepared by introducing CAA to the reducing end of cellulose. ^{1}H NMR for the obtained block copolymer indicated the presence of cellulose and PS bonded covalently to the cellulose. SEC traces for the obtained copolymer and kinetic study of polymerization suggested that our method was applicable to higher-molecular-weight cellulose (DP=250) and produced cellulose-*b*-PS with a predetermined molecular weight of PS block. Cellulose$_{250}$-*b*-PS, which was prepared with CuBr, exhibited narrow polydispersity. CuBr was more effective than CuCl in ATRP for cellulose-*b*-PS. Microscopic observation indicated that the addition of cellulose-*b*-PS enhanced the miscibility of the immiscible cellulose/PS blend. TG analysis of the blends showed reduced thermal stability and improved compatibility.

1 Yoshida, N., Kasuya, N., Haga, N. & Fukuda, K. Brand-new biomass-based vinyl polymers from 5-hydroxymethylfurfural. *Polym. J.* **40,** 1164–1169 (2008).
2 Chen, G. & Hoffman, A. S. Graft copolymers that exhibit temperature-induced phase transition over a wide range of pH. *Nature* **373,** 49–52 (1995).
3 Galaev, I. Y. & Mattiasson, B. Smart polymers and what they could do in biotechnology and medicine. *Trends Biotechnol.* **17,** 335–340 (1999).
4 Jeong, B., Bae, Y. H., Lee, D. S. & Kim, S. W. Biodegradable block copolymers as injectable drug-delivery systems. *Nature* **388,** 860–862 (1997).
5 Jeong, B. & Gutowska, A. Lessons from nature: stimuli-responsive polymers and their biomedical applications. *Trends Biotechnol.* **20,** 305–311 (2002).
6 Middleton, J. C. & Tipton, A. J. Synthetic biodegradable polymers as orthopedic devices. *Biomaterials* **21,** 2335–2346 (2000).
7 Patel, N., Padera, R., Sanders, G. H. W., Gannizzaro, S. M., Davies, M. C., Langer, R., Roberts, C. J., Tendler, S. J. B., Williams, P. M. & Shakesheff, K. M. Spatially controlled cell engineering on biodegradable polymer surfaces. *FASEB J.* **12,** 1447–1454 (1998).
8 Torchilin, V. P. Structure and design of polymeric surfactant-based drug delivery systems. *J. Controlled Release* **73,** 137–172 (2001).
9 Wagner, M. & Wolf, B. Effect of block copolymers on the interfacial tension between two immiscible homopolymers. *Polymer* **34,** 1460–1464 (1993).
10 Cigna, P., Favis, B. D. & Jerome, R. Diblock copolymers as emulsifying agents in polymer blends: influence of molecular weight, architecture, and chemical composition. *J. Polym. Sci., Part B: Polym. Phys.* **34,** 1691–1700 (1996).
11 Rösler, A., Vandermeulen, G. W. M. & Klok, H. A. Advanced drug delivery devices via self-assembly of amphiphilic block copolymers. *Adv. Drug Delivery. Rev.* **53,** 95–108 (2001).
12 Förster, S. & Antonietti, M. Amphiphilic block copolymers in structure-controlled nanomaterial hybrids. *Adv. Mater.* **10,** 195–217 (1998).
13 Enomoto, Y., Kamitakahara, H., Takano, T. & Nakatsubo, F. Synthesis of diblock copolymers with cellulose derivatives. 3. Cellulose derivatives carrying a single pyrene group at the reducing-end and fluorescent studies of their self-assembly systems in aqueous NaOH solutions. *Cellulose* **13,** 437–448 (2006).
14 Dou, H., Jiang, M., Peng, H., Chen, D. & Hong, Y. pH-dependent self-assembly: micellization and micelle-hollow-sphere transition of cellulose-based copolymers. *Angew. Chem. Int. Ed.* **42,** 1516–1519 (2003).
15 Kang, H., Liu, W., Liu, R. & Huang, Y. A novel, amphiphilic etyl cellulose grafting copolymer with poly(2-hydroxyethyl methacrylate) side chains and its micellization. *Macromol. Chem. Phys.* **209,** 424–430 (2008).
16 Nho, Y. C. & Kwon, O. H. Blood compatibility of AAc, HEMA, and PEGMA-grafted cellulose film. *Radiat. Phys. Chem.* **66,** 299–307 (2003).
17 Shen, D. & Huang, Y. The synthesis of CDA-*g*-PMMA copolymers through atom transfer radical polymerization. *Polymer* **45,** 7091–7097 (2004).

18 Shen, D., Yu, H. & Huang, Y. Densely grafting copolymers of ethyl cellulose through atom transfer radical polymerization. *J. Polym. Sci., Part A: Polym. Chem.* **43,** 4099–4108 (2005).
19 Wang, J. S. & Matyjaszewski, K. Controlled/living radical polymerization. Atom transfer radical polymerization in the presence of transition-metal complexes. *J. Am. Chem. Soc.* **117,** 5614–5615 (1995).
20 Wang, J. S. & Matyjaszewski, K. Controlled/living radical polymerization. Halogen atom transfer radical polymerization promoted by a Cu(I)/Cu(II) redox process. *Macromolecules* **28,** 7901–7910 (1995).
21 Kato, M., Sawamoto, M. & Higashimura, T. Polymerization of methyl methacrylate with the carbon tetrachloride/dichlorotris(triphenylphosphine)ruthenium(II)/Methylaluminum Bis(2,6-di-*tert*-butylphenoxide) initiating system: possibility of living radical polymerization. *Macromolecules* **28,** 1721–1723 (1995).
22 Braunecker, W. A. & Matyjaszewski, K. Controlled/living radical polymerization: features, developments, and perspectives. *Prog. Polym. Sci.* **32,** 93–146 (2007).
23 Coessens, V., Pintauer, T. & Matyjaszewski, K. Functional polymers by atom transfer radical polymerization. *Prog. Polym. Sci.* **26,** 337–377 (2001).
24 Matyjaszewski, K. Transition metal catalysis in controlled radical polymerization: atom transfer radical polymerization. *Chem. Eur. J.* **5,** 3095–3102 (1999).
25 Matyjaszewski, K. New materials by atom transfer radical polymerization. *Mol. Cryst. Li. Cryst.* **415,** 23–34 (2004).
26 Patten, T. E. & Matyjaszewski, K. Atom transfer radical polymerization and the synthesis of polymeric materials. *Adv. Mater.* **10,** 901–914 (1998).
27 Friedman, H. L. Kinetics of thermal degradation of char-forming plastics from thermogravimetry-application to a phenolic plastic. *J. Polym. Sci.* **C6,** 183–195 (1964).
28 Ozawa, T. A new method of analyzing thermogravimetric data. *Bull. Chem. Soc. Jpn.* **38,** 1881–1886 (1965).
29 Kissinger, H. E. Reaction kinetics in differential thermal analysis. *Anal. Chem.* **29,** 1702–1706 (1957).
30 Akahira, T. & Sunose, T. Trans. Joint convention of four electrical institutes. *Res. Rep. Chiba Inst. Technol.* **16,** 22–31 (1971).
31 Coats, A. W. & Redfern, J. P. Kinetic parameters from thermogravimetric data. *Nature* **201,** 68 (1964).
32 Isogai, A. & Usuda, M. Preparation of low-molecular weight cellulose using phosphoric acid. *Mokuzai. Gakkaishi.* **37,** 339–344 (1991).
33 Nishioka, N., Uno, M. & Ueda, A. Compatibility estimation in cellulosic blends by thermogravimetry. *Mem. Osaka Electro-Comm. Univ. Natur. Sci.* **41,** 89–94 (2006).
34 Pielichowski, K. & Fiejtuch, K. Non-oxidative thermal degradation of poly(ethylene oxide): kinetic and thermoanalytical study. *J. Anal. Appl. Pyrolysis* **73,** 131–138 (2005).
35 Barral, L., Diez, F. J., Garcia-Garbal, S., Lopez, J., Montero, B., Montes, R., Ramirez, C. & Rico, M. Thermodegradation kinetics of a hybrid inorganic-organic epoxy system. *Eur. Polym. J.* **41,** 1662–1666 (2005).
36 Meng, X., Huang, Y., Yu, H. & Lv, Z. Thermal degradation kinetics of polyimide containing 2,6-benzobisoxazole units. *Polym. Degrad. Stab.* **92,** 962–967 (2007).
37 Erceg, M., Kovacic, T. & Perinovic, S. Kinetic analysis of the non-isothermal degradation of poly(3-hydroxybutyrate) nanocomposites. *Thermochimica Acta.* **476,** 44–50 (2008).
38 Zhao, W., Zhang, Q., Chen, T. & Lu, T. Preparation and thermal decomposition of PS/Ni microspheres. *Mater. Chem. Phys.* **113,** 428–434 (2009).